



AHP–GIS and Sentinel-2 Remote Sensing for Landslide Susceptibility Mapping in Tipaza Province, Northern Algeria

Yamina Aoumer^{1*}, Mohamed.Said Guettouche^{2,3}, Mohand Ouabdallah Bounif¹, Leila Bouchama^{2,3},
Chahinez Alliche⁴, Asma Sebiat⁵, Zineb Haider⁴

¹ Department of Geophysics, Laboratory of Geophysics, Faculty of Earth Sciences, Geography and Regional Planning, University of Science and Technology Houari Boumediene, Bab Ezzouar 16024, Algeria

² Department of Geography and Regional Planning, Laboratory of Geomorphology and Geohazard, Faculty of Earth Sciences, Geography and Regional Planning, University of Science and Technology Houari Boumediene, Bab Ezzouar 16024, Algeria

³ Department of Geography and Regional Planning, Laboratory for Cities, Regions and Territorial Governance, Faculty of Earth Sciences, Geography and Regional Planning, University of Science and Technology Houari Boumediene, Bab Ezzouar 16024, Algeria

⁴ National Laboratory for Housing and Construction (NLHC)-General Directorate, Gué de Constantine 16042, Algeria

⁵ National Institute of Cartography and Remote Sensing, Hussein Dey 16005, Algeria

Corresponding Author Email: yaoumer@usthb.dz

Copyright: ©2026 The authors. This article is published by IETA and is licensed under the CC BY 4.0 license (<http://creativecommons.org/licenses/by/4.0/>).

<https://doi.org/10.18280/ijdne.210517>

ABSTRACT

Received: 4 March 2026
Revised: 16 May 2026
Accepted: 25 May 2026
Available online: 31 May 2026

Keywords:

landslide, remote sensing, Analytic Hierarchy Process, susceptibility, Geographic Information System

This study proposes an integrated spatial analysis framework for landslide susceptibility mapping in the Tipaza Province, northern Algeria. The methodology combines the Analytic Hierarchy Process (AHP) with geo-spatial factors processed using advanced geomatic modeling techniques. The susceptibility modeling integrates multiple geomorphological parameters within a Geographic Information System (GIS), including slope gradient, lithological units, Normalized Difference Vegetation Index (NDVI), Normalized Difference Water Index (NDWI), lineament density, drainage density, and topographic aspect. Data acquisition and processing relied on Sentinel-2 imagery with a 10 m spatial resolution for key bands, combined with the SRTM Digital Elevation Model, ensuring accurate spatial representation of terrain conditions. All thematic layers generated in ArcGIS were weighted according to their relative influence on gravitational slope instability, as determined by the AHP approach. The resulting susceptibility maps classify approximately 16.35% of the study area within high susceptibility zones. Validation through field investigations confirmed the model's reliability. The findings offer practical relevance for land-use planning and natural hazard management, while the proposed framework establishes a basis for complementary geophysical investigations and geological risk mitigation strategies.

1. INTRODUCTION

Landslides are one of the most destructive geological hazards worldwide, causing considerable human and economic losses [1, 2]. These gravitational instability phenomena particularly affect mountainous and coastal areas characterised by unstable slopes, where the mechanisms of failure are exacerbated by environmental and anthropogenic factors [3, 4]. These events are responsible for thousands of deaths each year and cause material damage estimated at several billion dollars.

Assessing susceptibility to landslides is a fundamental step in the preventive management of natural hazards and land use planning [5, 6]. This assessment requires the integration of multiple geomorphological parameters, including slope, lithology, lineament density, slope orientation, and hydrographic network density, all of which are recognised as determining factors in slope instability dynamics [7, 8].

Significant methodological advances have been made over the last decade, particularly in the integration of multi-criteria analytical methods into Geographic Information Systems (GIS) [9]. Analytic Hierarchy Process (AHP), initially developed by Saaty [10], has proven particularly effective in weighting the various factors contributing to susceptibility [5, 11]. This approach, combined with the use of remote sensing data, has proven its reliability in various regional studies in Asia and Latin America [12-14].

The Tipaza region, located on the northern coast of Algeria, has a geomorphological context conducive to slope instability due to its rugged topography, varied lithology, and Mediterranean climatic conditions characterised by intense rainfall events. Increasing urbanisation and anthropogenic landscape changes have potentially amplified the vulnerability of the territory [15]. Despite these predispositions, few systematic studies have been conducted to map landslide susceptibility in this region.

This study aims to develop a methodology for assessing landslide susceptibility in Tipaza, based on the integration of AHP and remote sensing data in a GIS environment. The specific objectives include:

- Identifying and prioritising factors predisposing landslides in the regional context,
- Developing a high spatial resolution susceptibility map, and
- This research validates the model through field observations. In addition, it lays the groundwork for subsequent geophysical investigations, allowing for a more in-depth characterisation of instability mechanisms.

The methodological approach incorporates indices derived from satellite imagery, including the Normalized Difference Vegetation Index (NDVI) and the Normalized Difference Water Index (NDWI), to assess the influence of vegetation cover and soil moisture on slope stability [16]. The results of this study will contribute significantly to the development of risk mitigation strategies and the optimisation of land-use planning in the region.

2. MATERIALS AND METHODS

2.1 Study area

The Tipaza Province is located in the northern part of the central Tell region of Algeria and is bordered by several administrative provinces (Figure 1). To the north, it is bounded by the Mediterranean Sea, while Chlef Province lies to the

west. Ain Defla Province and Blida Province border Tipaza to the southwest and south, respectively, whereas Algiers Province forms their eastern boundary. This geographical position (Longitude: 1.64399° E-2.83420° E, Latitude: 36.35625° N-36.70015° N) places Tipaza Province at the interface of diverse natural landscapes and socio-economic influences.

Covering an area of approximately 2,000 km², the region is characterised by a complex and rugged topography dominated by the Sahel anticline, Mount Chenoua, and the eastern Dahra range. Elevations range from sea level to approximately 1,100 m, conferring a distinctive geomorphological setting and significant touristic potential. In addition, the province hosts a rich historical heritage and numerous infrastructural developments.

According to the General Population and Housing Census (RGPH), the province recorded 591,010 inhabitants in 2008. The preliminary census of 2022 registered 616,150 inhabitants, reflecting a growth rate of approximately 0.27% per year over the 14-year intercensal period, a relatively moderate demographic increase indicative of stable but slow population dynamics.

The coastline extends for nearly 123 km and includes a wide variety of beaches, coves, bays, and cliffs, offering favorable conditions for coastal tourism and related economic activities. In recent years, Tipaza Province has experienced rapid urban expansion accompanied by the development of new infrastructure and land-use changes, which have significantly transformed the landscape and increased pressure on the natural environment.

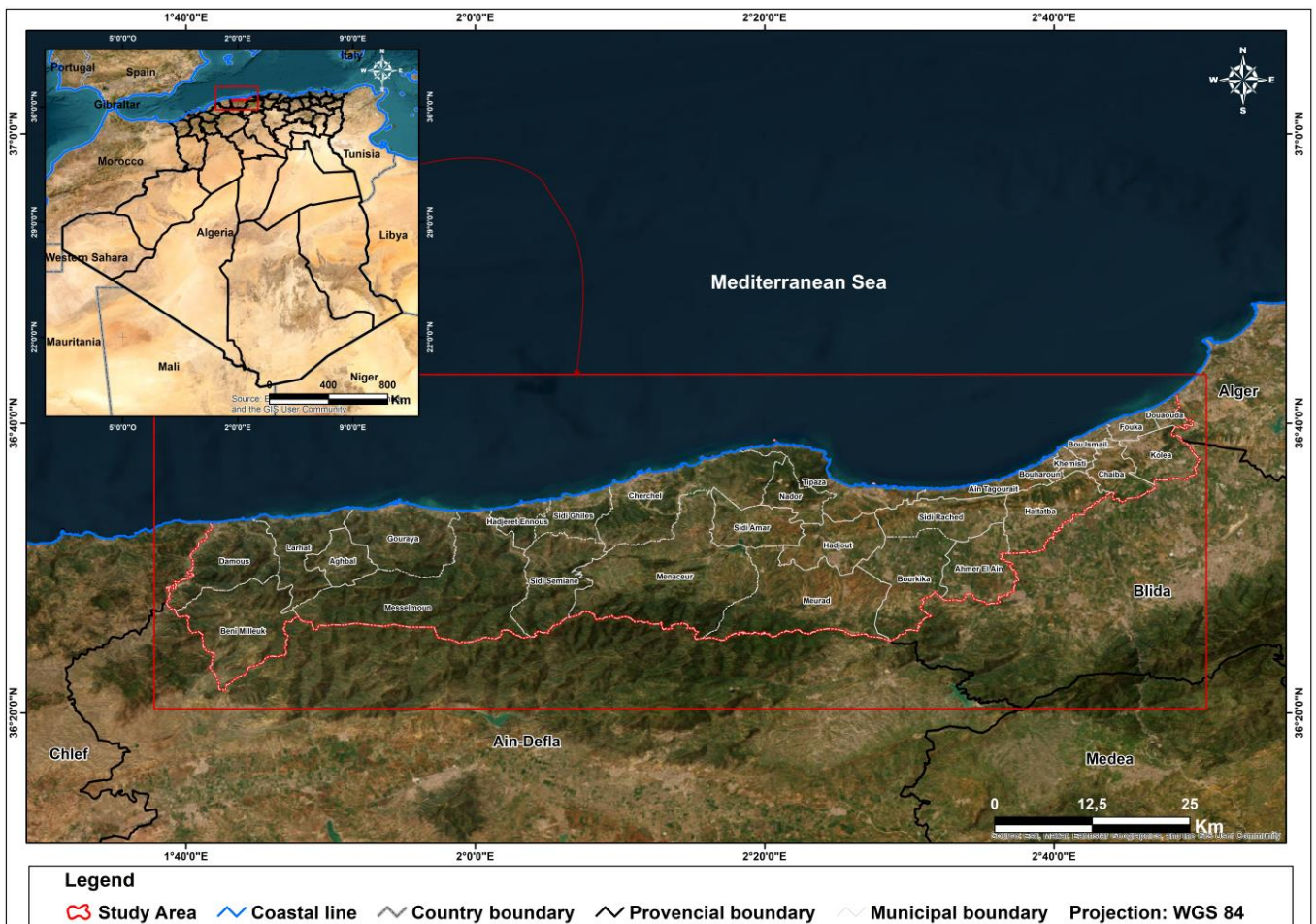


Figure 1. Location of the study area

2.2 Workflow of landslide susceptibility

Initially, landslide inventorying and characterization were conducted through the analysis of thematic maps, satellite imagery, and field surveys. This phase facilitated the identification and selection of the principal factors controlling landslide occurrence within the study area, based on both empirical observations and a comprehensive review of relevant scientific literature.

Subsequently, the AHP was employed to organize the selected landslide conditioning factors into a hierarchical structure and to determine their relative weights according to their respective influence on slope instability.

2.3 Data sources and preprocessing

Sentinel-2 Level-2A multispectral images were acquired from the Copernicus Open Access Hub [17], and two cloud-free scenes dated April 16 and April 18, 2024, were selected for analysis. Image preprocessing was performed using the Sentinel Application Platform (SNAP), where all spectral bands were resampled to a common spatial resolution to ensure consistency for subsequent spatial and spectral analyses. In parallel, a Digital Elevation Model (DEM) derived from the Shuttle Radar Topography Mission (SRTM) was obtained from the United States Geological Survey (USGS) [18]. The original 30-m resolution DEM was resampled to 10 m using ArcGIS 10.8 software to ensure spatial compatibility with the satellite imagery and to support detailed terrain analyses. The satellite imagery was pre-processed and analyzed using ENVI software. Both datasets were subsequently integrated within a GIS environment to facilitate the extraction of geomorphological parameters and the implementation of landslide susceptibility modelling.

2.4 Predisposing factors

This study focuses on the spatial component of landslide susceptibility; therefore, only the predisposing factors were considered and mapped. The predictors used for landslide susceptibility modelling include lithology (LT), drainage density (DD), slope (SL), lineament density (LD), aspect (AS), the NDVI, and the NDWI. These factors were selected because they represent the main geological, topographical, hydrological, and land-cover conditions influencing landslide occurrence in the study area.

2.4.1 Lithology

Lithology (LT) is a primary factor influencing slope stability (Figure 2). To develop a lithology map of the study area, two regional geological maps at a scale of 1:200,000, covering the Blida and Chlef provinces, were digitized. Information regarding rock type, age, and stratigraphy was compiled, and a classification system consisting of five lithological categories was established, taking into account field geological evidence.

The occurrence and spatial distribution of the geological units identified in the study area reveal that distinct formations dominate different sectors. Lithological information at the regional scale was extracted using geological maps, satellite imagery, and professional GIS software. The resulting map (Figure 2) highlights three major lithological classes: marls and clays (yellow zone), tuffs and lava flows (dark green), and andesite (light green). Marls and clays are distinguished by their relatively low shear strength and susceptibility to slope instability, whereas volcanic units, including tuffs, lava flows, and andesite, represent more resistant lithologies that define contrasting geomorphological patterns.

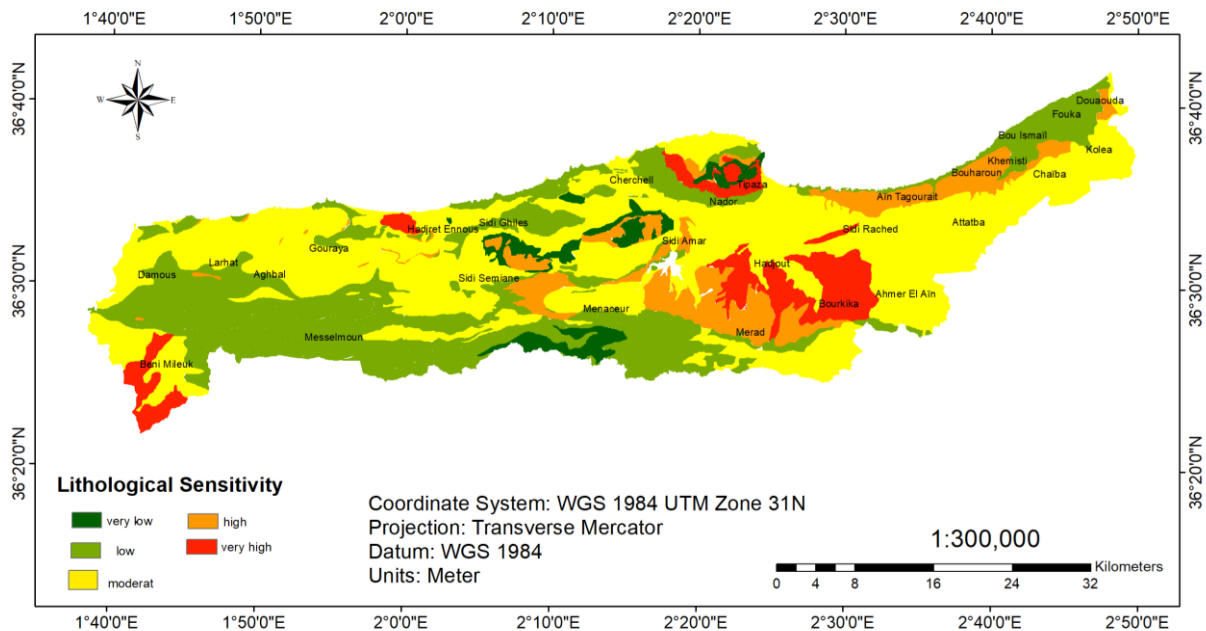


Figure 2. Lithology map

2.4.2 Lineament density

To generate a lineament and lineament density map using PCI 8-bit grayscale images with a spatial resolution of 10 meters, we used ENVI 5.1, PCI Geomatica 2013, and ArcMap 10.8 (Figure 3). The process began with importing the

grayscale images into ENVI 5.1 for Gram-Schmidt Sharpening (GSS) to enhance spatial resolution by combining high-resolution panchromatic images with multispectral data. This enhanced image was processed in PCI Geomatica 2013 to detect and extract lineaments using edge detection

algorithms. These lineaments were then digitized [10, 11], exported to ArcMap 10.8, and used to create a lineament density map by calculating lineament frequency within specified grid cells. The final steps involved exporting the lineaments as a CAD file, importing it into ArcMap, converting CAD lines to a shapefile, symbolizing the lineaments, and classifying the lineament density map into five

classes using the "line Density" tool from the Spatial Analyst toolbox (Figure 3).

Along the coast, lineament density is low to moderate, indicating stable geological conditions with fewer fractures. In the eastern regions, lineament density is high to very high, reflecting significant geological fracturing and potential fault zones due to tectonic movements.

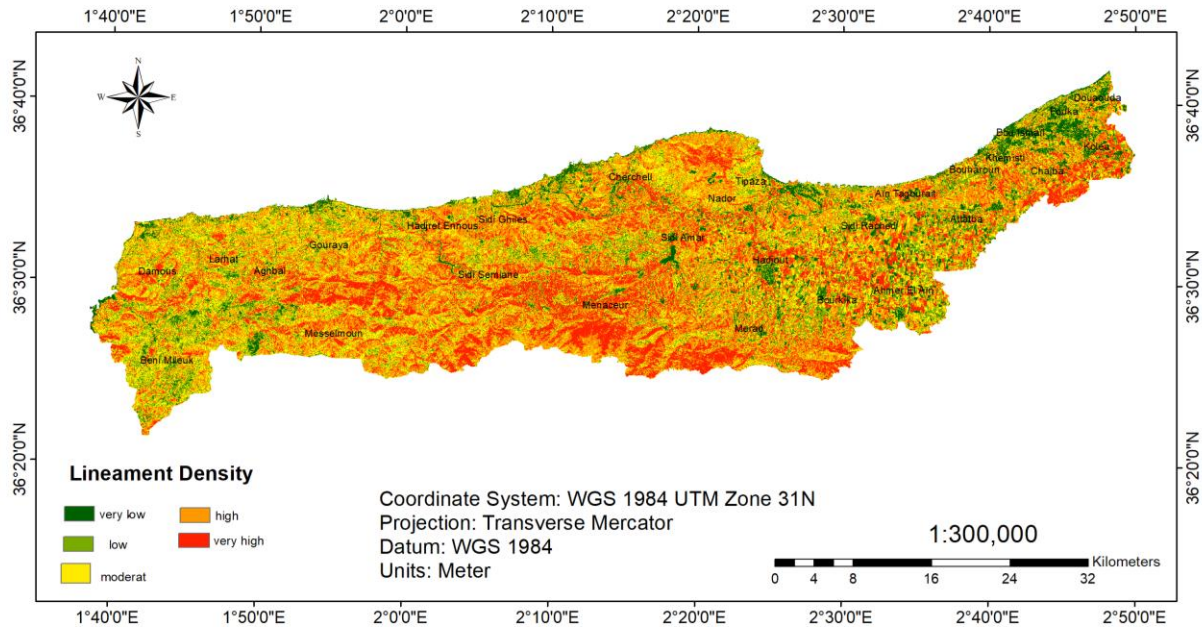


Figure 3. Lineament and density map

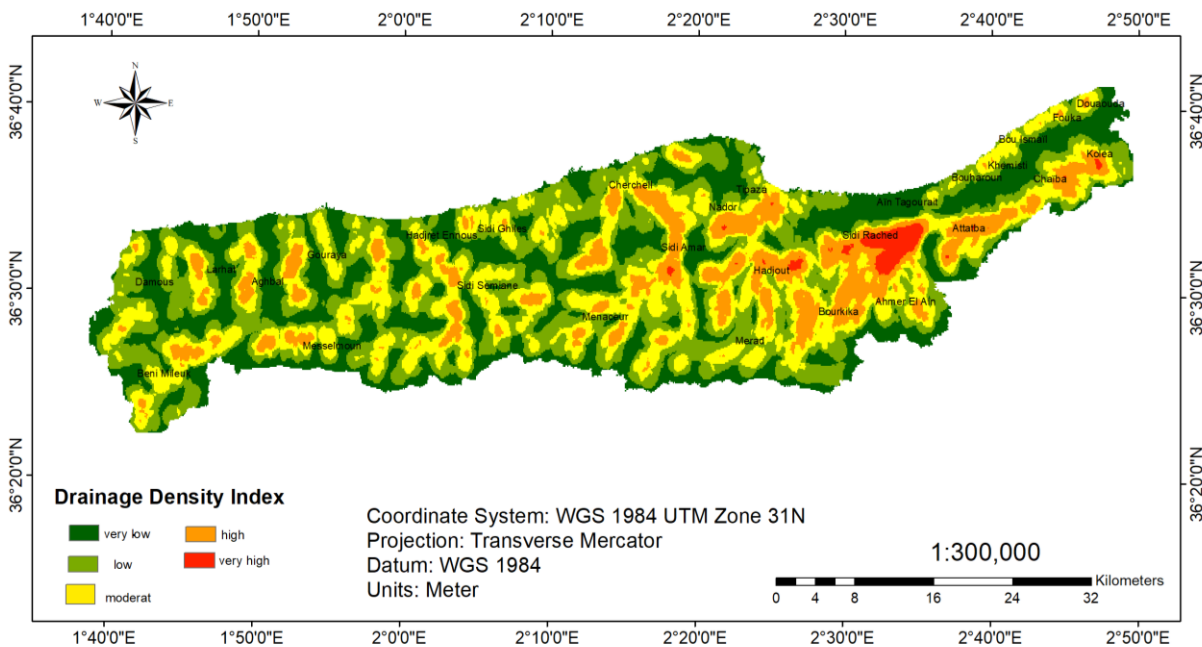


Figure 4. Drainage density map

2.4.3 Drainage density

Along the coast, the terrain is generally flat, with less extensive drainage networks, resulting in low to moderate density (Figure 4). In the eastern regions, the terrain is complex with well-established drainage networks, indicating a high to very high density likely due to significant rainfall and steep slopes.

2.4.4 Aspect

Aspect refers to the direction that a slope faces relative to the sun. Aspect influences factors such as solar radiation, temperature variation, and moisture distribution, which can affect slope stability. While aspect contributes to landslide susceptibility, its influence is relatively lower compared to other factors.

Diverse Slope Orientations: The map (Figure 5) reveals a varied distribution of slope orientations across the region. The coastal area shows a mix of slopes predominantly facing north, northeast, and northwest, which are typical in coastal and mountainous terrains. The central and southern parts of the Province exhibit a mix of slopes facing all directions, indicating a highly varied topography. The prevalence of southeast and southwest-facing slopes in certain areas suggests significant solar exposure and potential impacts on vegetation and soil moisture. Areas with a high concentration

of slopes facing south, southeast, and southwest may be more susceptible to landslides due to increased weathering and erosion from sun exposure and prevailing wind directions.

2.4.5 Normalized Difference Vegetation Index

NDVI measures the density and health of vegetation cover. Vegetation helps stabilize slopes by reducing soil erosion and enhancing soil cohesion. Areas with dense vegetation cover are less susceptible to landslides compared to areas with sparse or no vegetation (Figure 6).

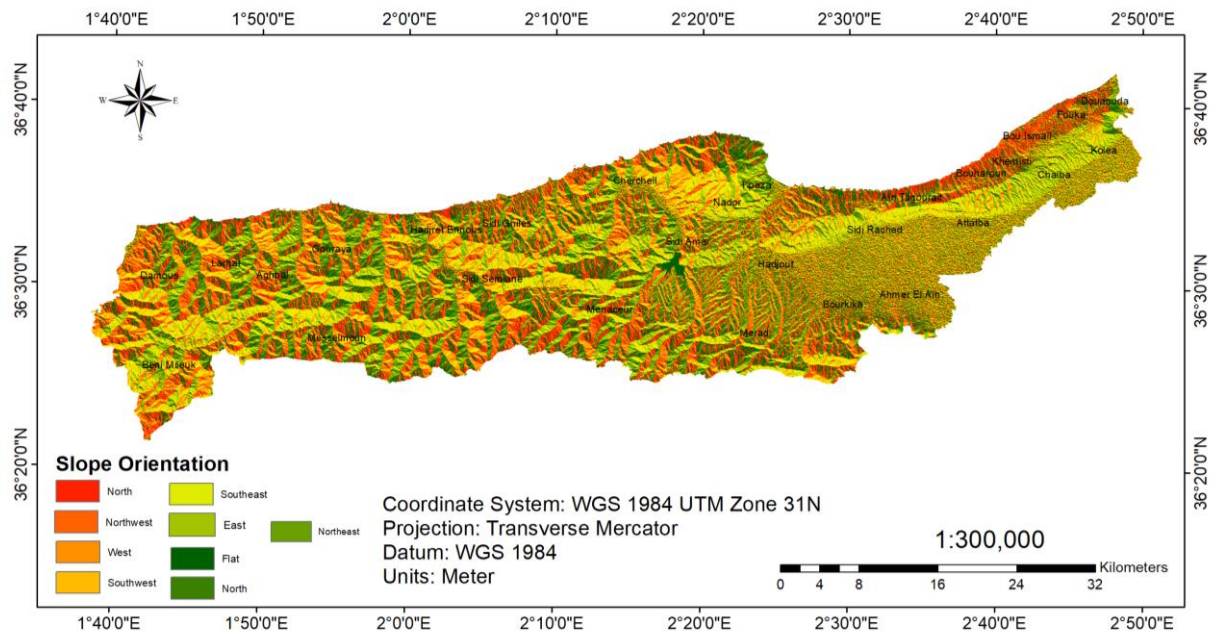


Figure 5. Slope orientation map (Aspect)

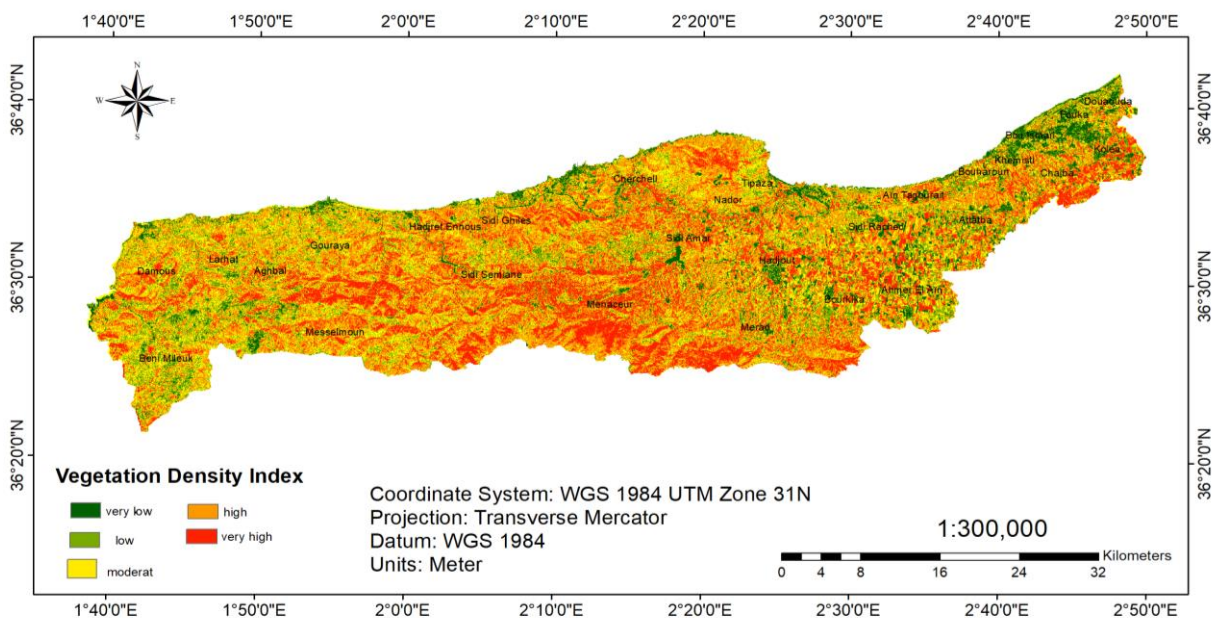


Figure 6. Normalized Difference Vegetation Index (NDVI) map

2.4.6 Normalized Difference Water Index

The NDVI and NDWI maps were generated using Sentinel-2 imagery processed in ENVI and ArcMap. NDVI reflects vegetation cover and its stabilizing role on slopes (Figure 6), while NDWI (Figure 7) represents soil moisture content,

which can reduce slope stability and increase landslide susceptibility, particularly during periods of heavy rainfall. In the analysis. Both indices were classified into five classes and integrated into the landslide susceptibility assessment.

The first step of the AHP approach consists in organizing the decision problem into a clear hierarchical structure. This hierarchy is generally composed of three levels:

- the overall objective, which in this case is landslide susceptibility assessment;
- the evaluation criteria, representing the selected conditioning factors; and
- the sub-criteria, corresponding to the different classes or categories of each factor.

This hierarchical organization helps to simplify the problem and facilitates a systematic comparison between factors [19].

Once the hierarchy is defined, the relative importance of the criteria is evaluated through pairwise comparisons. Each criterion C_i is compared with another criterion C_j . The outcome of each comparison is expressed by a numerical value a_{ij} , indicating how much more important C_i is compared to C_j , based on expert judgment and knowledge of landslide processes [20].

All pairwise comparisons are then organized into a square reciprocal matrix A of order n , where $a_{ij} = 1/a_{ji}$ and $a_{ii} = 1$. To make the values comparable, the comparison matrix is normalized by dividing each element by the sum of its corresponding column [11, 21].

$$A = \begin{bmatrix} 1 & a_{12} & \dots & a_{1n} \\ \frac{1}{a_{12}} & 1 & \dots & a_{2n} \\ \vdots & \vdots & \ddots & \vdots \\ \frac{1}{a_{1n}} & \frac{1}{a_{2n}} & \dots & 1 \end{bmatrix}$$

The relative weight w_i of each criterion is then obtained by calculating the average of the normalized values in each row [19, 21].

$$W_i = \sum_{j=1}^n \bar{a}_{ij}$$

The resulting weight vector satisfies the condition

$$\sum_{i=1}^n W_i = 1$$

To ensure that the pairwise comparisons are logically consistent, a consistency analysis is performed.

The maximum eigenvalue λ_{max} of the comparison matrix is computed, and the Consistency Index (CI) is defined as [21].

$$CI = \frac{\lambda_{max} - n}{n - 1}$$

The Consistency Ratio (CR) is then calculated as [21, 22].

$$CR = \frac{CI}{RI}$$

where, RI represents the Random CI. A matrix is considered acceptable when $CR < 0.10$, indicating reliable expert judgments [19].

The same AHP procedure is applied to the sub-criteria associated with each main factor. Pairwise comparisons are

conducted within each criterion to derive local weights, which are then multiplied by the corresponding criterion weight to obtain global weights [20]. Finally, the AHP-derived weights are integrated into the GIS environment using a weighted linear combination (WLC) approach to compute the landslide susceptibility index [23].

$$LSI = \sum_{i=1}^n w_i * x_i$$

where, w_i denotes the weight of the criterion i and x_i represents the standardized spatial value of the corresponding factor. This formulation enables the transformation of the AHP decision model into a continuous spatial representation suitable for landslide susceptibility mapping and land-use planning [11].

3. RESULTS AND DISCUSSION

3.1 Conditioning factor weighting results

Data related to each landslide conditioning factor, including slope, lineament density, drainage density, lithology, aspect, the NDVI, and the NDWI, were collected and analysed concurrently. These datasets (Table 1) were processed to generate spatial layers within a GIS environment for subsequent landslide susceptibility mapping. The relative importance of the selected criteria was then assessed using the AHP, whereby pairwise comparisons were conducted among all criteria to establish their hierarchical relationships. This comparative evaluation enabled the systematic weighting of factors based on their contribution to slope instability.

Once the pairwise comparisons are validated and consistent, the weights for each criterion are calculated using AHP's mathematical algorithms. These weights (Table 2) reflect the relative importance of each criterion in determining landslide susceptibility. ArcGIS is used for spatial analysis, meticulously processing geospatial data to create thematic maps for factors like slope gradients, lineament densities, and lithological characteristics. Our approach involved rigorous data preprocessing and the integration of remote sensing imagery and topographic data.

The combined analysis of the pairwise comparison matrix (Table 1) and the AHP-derived weights (Table 2) reveals a coherent eco-geomorphological structure controlling landslide susceptibility. The interaction patterns (Table 1) show a strongly coupled morphostructural system composed of slope (SL), lineament density (LD), and drainage density (DD), characterized by equal relative importance (1.000), indicating their joint control on terrain organization and gravitational energy distribution. Lithology (LT) exhibits consistently high associations with these variables (0.857), reflecting its role as a mechanical and structural mediator between bedrock conditions and surface processes. NDVI and NDWI are perfectly correlated (1.000), highlighting their integrated representation of eco-hydrological conditions, while their moderate links with other factors (0.714–0.833) indicate a regulating function in moisture and vegetation-driven slope stability. Aspect (AS) shows the weakest relationships (0.429–0.600), confirming a secondary influence mainly related to microclimatic effects.

The AHP results (Table 2) confirm this structure by

quantifying factor importance. Slope (SL), lineament density (LD), and drainage density (DD) dominate the system with identical highest weights ($W_i = 0.175$; Rank = 1), emphasizing their primary role in controlling slope instability. Lithology (LT) occupies an intermediate position ($W_i = 0.150$; Rank = 4), acting as a litho-mechanical control linking structure and surface response. NDVI and NDWI show equal importance ($W_i = 0.125$; Rank = 5), reflecting their coupled eco-hydrological regulation of moisture and vegetation effects on slope stability. Aspect (AS) has the lowest contribution ($W_i = 0.075$; Rank = 7), indicating a limited role in comparison to other conditioning factors.

The consistency values ($n = 7$; $\lambda_{max} = 7.01$; $CI = 0.00167$; $RI = 1.32$; $CR = 0.00126$) confirm the reliability of the AHP framework. Since the CR value is well below the acceptable threshold of 0.1, the pairwise comparison matrix is considered highly consistent, supporting the robustness of the weighting procedure.

Overall, landslide susceptibility in the study area results from a hierarchical interaction where morphostructural factors dominate, lithology acts as a coupling interface, and eco-hydrological variables provide environmental regulation, while aspect plays a secondary role.

Table 1. Pairwise comparison matrix of landslide conditioning factors

| Factors | SL | LD | DD | LT | NDVI | NDWI | AS |
|---------|-------|-------|-------|------|-------|-------|------|
| SL | 1 | 1 | 1 | 0.86 | 0.71 | 0.71 | 0.43 |
| LD | 1 | 1 | 1 | 0.86 | 0.71 | 0.71 | 0.43 |
| DD | 1 | 1 | 1 | 0.86 | 0.71 | 0.71 | 0.43 |
| LT | 1.167 | 1.167 | 1.167 | 1 | 0.83 | 0.83 | 0.5 |
| NDVI | 1.4 | 1.4 | 1.4 | 1.2 | 1 | 1 | 0.6 |
| NDWI | 1.4 | 1.4 | 1.4 | 1.2 | 1 | 1 | 0.6 |
| AS | 2.33 | 2.33 | 2.33 | 2 | 1.167 | 1.167 | 1 |

Note: SL: slope, LD: lineament density, DD: drainage density, LT: lithology, NDVI: Normalized Difference Vegetation Index, NDWI: Normalized Difference Water Index, AS: aspect.

Table 2. Pairwise comparison matrix of conditioning factors, AHP-derived weights, and ranking

| Factors | SL | LD | DD | LT | NDVI | NDWI | AS | W_i | Rank |
|---------|-------|-------|-------|------|-------|-------|------|-------|------|
| SL | 1 | 1 | 1 | 0.86 | 0.71 | 0.71 | 0.43 | 0.175 | 1 |
| LD | 1 | 1 | 1 | 0.86 | 0.71 | 0.71 | 0.43 | 0.175 | 1 |
| DD | 1 | 1 | 1 | 0.86 | 0.71 | 0.71 | 0.43 | 0.175 | 1 |
| LT | 1.167 | 1.167 | 1.167 | 1 | 0.83 | 0.83 | 0.50 | 0.150 | 4 |
| NDVI | 1.4 | 1.4 | 1.4 | 1.2 | 1 | 1 | 0.60 | 0.125 | 5 |
| NDWI | 1.4 | 1.4 | 1.4 | 1.2 | 1 | 1 | 0.60 | 0.125 | 5 |
| AS | 2.33 | 2.33 | 2.33 | 2 | 1.167 | 1.167 | 1 | 0.075 | 7 |

Note: SL: slope, LD: lineament density, DD: drainage density, LT: lithology, NDVI: Normalized Difference Vegetation Index, NDWI: Normalized Difference Water Index, AS: aspect. Parameters: $n = 7$, $\lambda_{max} = 7.01$, $CI = 0.00167$, $RI = 1.32$, $CR = 0.00126$ (0.126%).

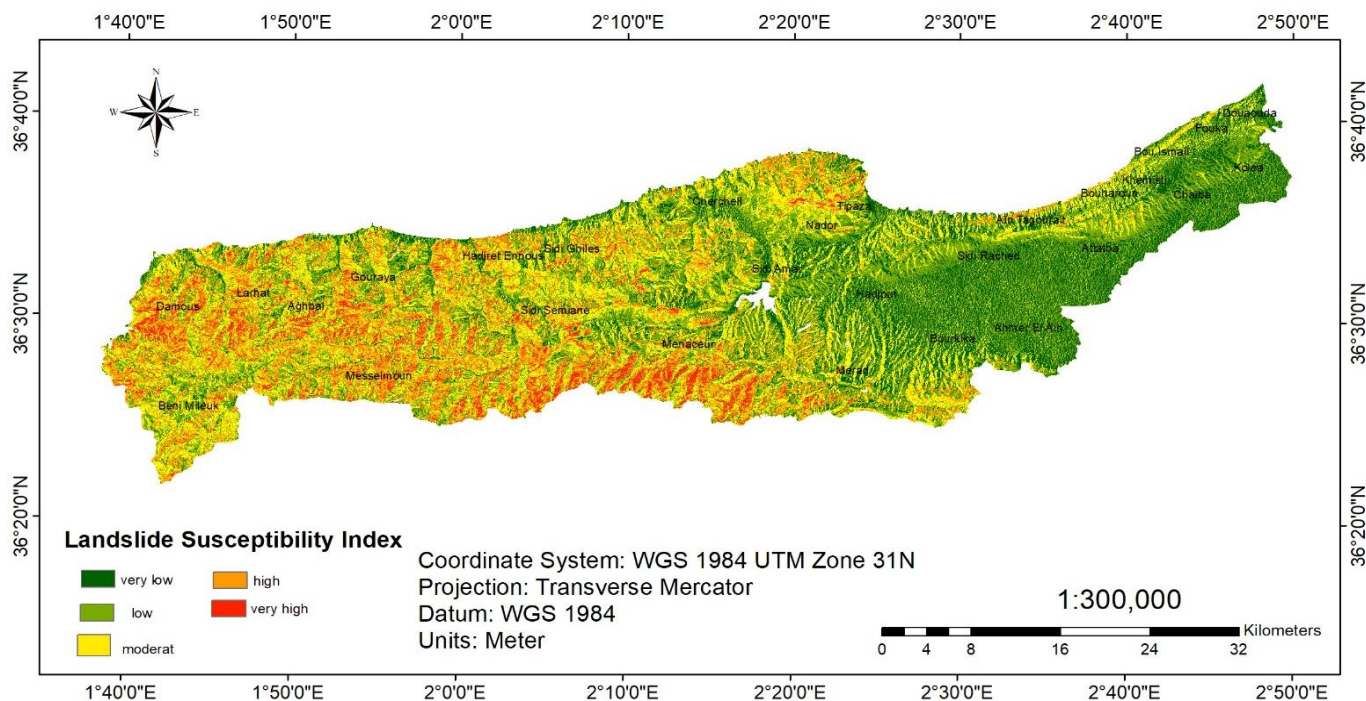


Figure 9. Susceptibility to landslides map

3.2 Spatial distribution of landslide susceptibility classes

The landslide susceptibility map (Figure 9) derived from the AHP delineates the Wilaya of Tipaza into five discrete susceptibility classes, ranging from very low to very high. Spatial analysis of the resulting distribution reveals a pronounced geographic differentiation: the eastern sector of the study area is predominantly characterized by low susceptibility values, reflecting comparatively stable geomorphological and lithological conditions. Conversely, the western and southwestern portions exhibit elevated susceptibility levels, classified as high to very high, attributable to the convergence of several predisposing factors, including pronounced topographic gradients, high drainage density, well-developed lineament networks, and unfavorable geological configurations.

3.3 Field observations

During our trip to the Tipaza area, several landslides were identified along the road and the coast (Figure 10). The wilaya

of Tipaza is served by a hierarchical road network comprising national roads, wilaya roads, and communal roads, ensuring connectivity across the province and with neighbouring regions.

The coastal road constitutes the main axis linking the province eastward to Algiers and westward to Cherchell, while the East-West highway further enhances regional accessibility, although some inland and mountainous areas remain poorly connected due to the rugged terrain. Field observations conducted along the coastal road identified several landslide occurrences that spatially correspond to zones classified as low, moderate, and high susceptibility on the landslide susceptibility map. The susceptibility assessment indicates that 19.66% and 31.78% of the study area are characterized by very low and low susceptibility classes, respectively; 27.20% and 16.35% correspond to moderate and high susceptibility classes, respectively; while 5.02% of the study area is characterized by very high susceptibility. These results highlight the relevance of the approach as a valuable tool for landslide prediction, territorial planning, and the development of mitigation and monitoring strategies across the study area.

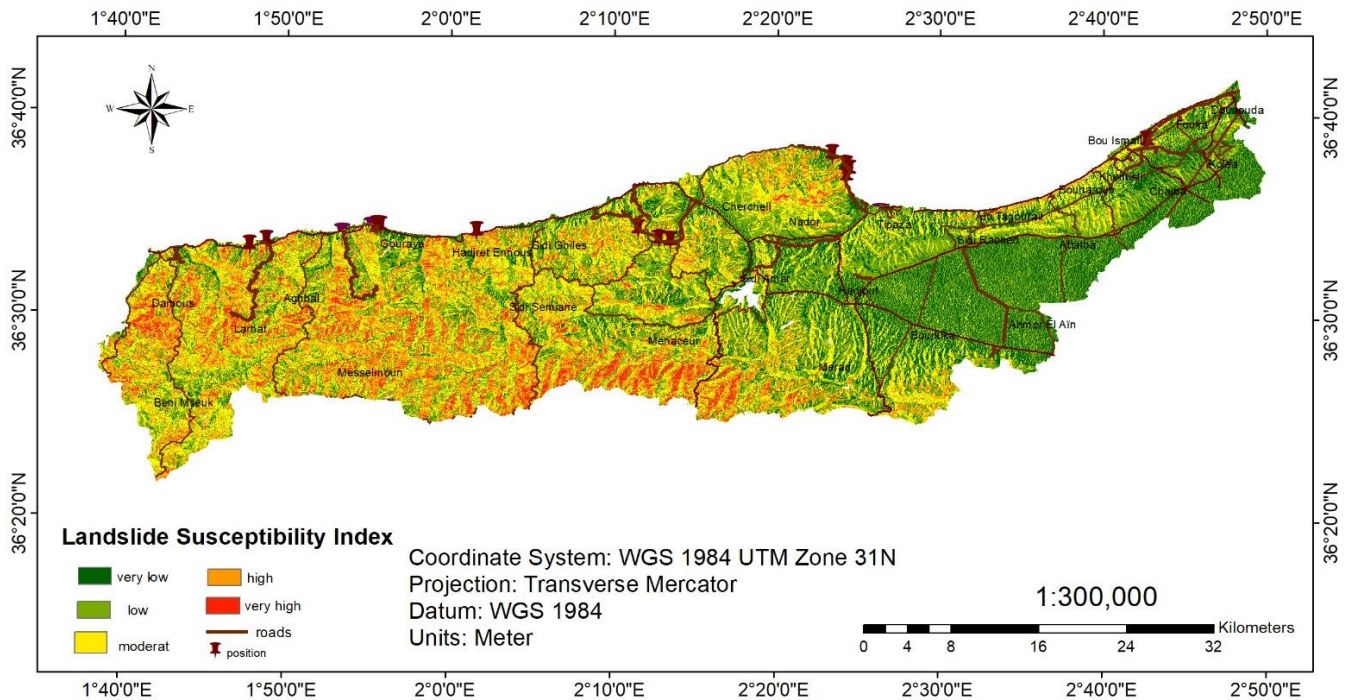


Figure 10. Field validation of landslides

4. CONCLUSION

This study demonstrates that the integration of the AHP with remote sensing and GIS techniques constitutes a framework for landslide susceptibility assessment in the Tipaza region, northern Algeria. By systematically applying pairwise comparisons, key landslide conditioning factors namely slope, lineament density, drainage density, lithology, aspect, NDVI, and NDWI; were objectively weighted, allowing for the generation of accurate and detailed susceptibility maps that reflect the combined influence of topographic, geological, and environmental conditions.

The use of Sentinel-2 imagery, coupled with terrain parameters derived from the SRTM Digital Elevation Model,

significantly enhanced the spatial characterization of slope instability and landscape dynamics. The resulting landslide susceptibility maps effectively delineate zones exposed to varying levels of landslide and were validated through field observations and comparison with existing datasets, confirming the reliability of the adopted methodology.

The outcomes of this research provide valuable insights for land-use planning and infrastructure development strategies in the Tipaza region. Furthermore, the proposed methodological framework offers a transferable and cost-effective approach that can be applied to other regions with similar geomorphological and geological settings. Continued refinement of the model through the integration of additional temporal triggering factors and updated datasets would further

improve its predictive capability and contribute to strengthening regional resilience and sustainable development.

ACKNOWLEDGMENT

The authors would like to express their appreciation for the help, support, and encouragement of all those who contributed to the preparation of the present work.

REFERENCES

- [1] Petley, D. (2012). Global patterns of loss of life from landslides. *Geology*, 40(10): 927-930. <https://doi.org/10.1130/G33217.1>
- [2] Alcántara-Ayala, I. (2025). Landslides in a changing world. *Landslides*, 22(9): 2851-2865. <https://doi.org/10.1007/s10346-024-02451-1>
- [3] Van Asch, T.W., Malet, J.P., Bogaard, T.A. (2009). The effect of groundwater fluctuations on the velocity pattern of slow-moving landslides. *Natural Hazards and Earth System Sciences*, 9(3): 739-749. <https://doi.org/10.5194/nhess-9-739-2009>
- [4] Crozier, M.J. (2010). Deciphering the effect of climate change on landslide activity. *Geomorphology*, 124(3-4): 260-267. <https://doi.org/10.1016/j.geomorph.2010.04.009>
- [5] Thammaboribal, P., Triapthti, N.K., Lipiloet, S. (2025). Using of analytical hierarchy process (AHP) in disaster management: A review of flooding and landslide susceptibility mapping. *International Journal of Geoinformatics*, 21(4): 177-196. <https://doi.org/10.52939/ijg.v21i4.4091>
- [6] Fell, R., Corominas, J., Bonnard, C., Cascini, L., Leroi, E., Savage, W.Z. (2008). Guidelines for landslide susceptibility, hazard and risk zoning for land use planning. *Engineering Geology*, 102(3-4): 85-98. <https://doi.org/10.1016/j.enggeo.2008.03.022>
- [7] Ghimire, M. (2011). Landslide occurrence and its relation with terrain factors in the Siwalik Hills, Nepal: Case study of susceptibility assessment in three basins. *Natural Hazards*, 56(1): 299-320. <https://doi.org/10.1007/s11069-010-9569-7>
- [8] Guzzetti, F., Carrara, A., Cardinali, M., Reichenbach, P. (1999). Landslide hazard evaluation: A review of current techniques and their application in a multi-scale study, Central Italy. *Geomorphology*, 31(1-4): 181-216. [https://doi.org/10.1016/S0169-555X\(99\)00078-1](https://doi.org/10.1016/S0169-555X(99)00078-1)
- [9] Seddiki, A., Dehimi, S. (2022). Using GIS combined with AHP for mapping landslide susceptibility in Mila, in Algeria. *International Journal of Design & Nature and Ecodynamics*, 17(2): 169-175. <https://doi.org/10.18280/ijdne.170202>
- [10] Zhang, X.K., Shao, S., Shao, S. (2024). Landslide susceptibility zonation using the Analytical Hierarchy Process (AHP) in the Great Xi'an Region, China. *Scientific Reports*, 14: 2941. <https://doi.org/10.1038/s41598-024-53630-y>
- [11] Malczewski, J. (1999). *GIS and Multicriteria Decision Analysis*. John Wiley & Sons, New York.
- [12] Du, G., Zhang, Y., Yang, Z., Guo, C., Yao, X., Sun, D. (2019). Landslide susceptibility mapping in the region of eastern Himalayan syntaxis, Tibetan Plateau, China: A comparison between analytical hierarchy process information value and logistic regression-information value methods. *Bulletin of Engineering Geology and the Environment*, 78(6): 4201-4215. <https://doi.org/10.1007/s10064-018-1393-4>
- [13] Shahabi, H., Hashim, M. (2015). Landslide susceptibility mapping using GIS-based statistical models and remote sensing data in tropical environment. *Scientific Reports*, 5: 9899. <https://doi.org/10.1038/srep09899>
- [14] Valqui-Reina, S.V., García-Naranjo, L.F. (2025). Geospatial landslide risk mapping using AHP and GIS: A case study of the Utcubamba River Basin, Peru. *Applied Sciences*, 15(17): 9423. <https://doi.org/10.3390/app15179423>
- [15] Skilodimou, H.D., Bathrellos, G.D., Koskeridou, E., Soukis, K., Rozos, D. (2018). Physical and anthropogenic factors related to landslide activity in the northern Peloponnese, Greece. *Land*, 7(3): 85. <https://doi.org/10.3390/land7030085>
- [16] Aslam, B., Maqsoom, A., Khalil, U., Ghorbanzadeh, O., Blaschke, T., Farooq, D., Tufail, R.F., Suhail, S.A., Ghamisi, P. (2022). Evaluation of different landslide susceptibility models for a local scale in the Chitral District, Northern Pakistan. *Sensors*, 22(9): 3107. <https://doi.org/10.3390/s22093107>
- [17] Ecosystem, C.D.S. (2023). Copernicus data space ecosystem. <https://dataspace.copernicus.eu>
- [18] Baker, M. (1895). The US geological survey. *The Geographical Journal*, 6(3): 252-260. <https://doi.org/10.2307/1774250>
- [19] Saaty, T.L. (2008). Decision making with the analytic hierarchy process. *International Journal of Services Sciences*, 1(1): 83-98. <https://doi.org/10.1504/IJSSCI.2008.017590>
- [20] Kayastha, P., Dhital, M.R., De Smedt, F. (2013). Application of the analytical hierarchy process (AHP) for landslide susceptibility mapping: A case study from the Tinau watershed, west Nepal. *Computers & Geosciences*, 52: 398-408. <https://doi.org/10.1016/j.cageo.2012.11.003>
- [21] Saaty, T.L., Wind, Y. (1980). Marketing applications of the analytic hierarchy process. *Management Science*, 26(7): 641-658. <https://doi.org/10.1287/mnsc.26.7.641>
- [22] Alonso, J.A., Lamata, M.T. (2006). Consistency in the analytic hierarchy process: A new approach. *International Journal of Uncertainty, Fuzziness and Knowledge-Based Systems*, 14(4): 445-459. <https://doi.org/10.1142/S0218488506004114>
- [23] Eastman, J.R. (1999). Multi-criteria evaluation and GIS. *Geographical Information Systems*, 1(1): 493-502. https://www.geos.ed.ac.uk/~gisteac/gis_book_abridged/files/ch35.pdf